JOURNAL OF CATALYSIS 140, 30–40 (1993)

Stereoselective Thymol Hydrogenation

I. Kinetics of Thymol Hydrogenation on Charcoal-Supported Platinum Catalysts

MICHÈLE BESSON,[1] LOUISE BULLIVANT, NATHALIE NICOLAUS, AND PIERRE GALLEZOT

Institut de Recherches sur la Catalyse-CNRS, 2 avenue Albert Einstein, 69626 Villeurbanne Cedex, France

Received February 28, 1992; revised October 29, 1992

The kinetics of thymol hydrogenation on a well-characterized supported platinum catalyst have been investigated in cyclohexane at temperatures between 313 and 373 K and under 3 MPa of hydrogen pressure. The relative rate constants of the different reaction pathways (hydrogenation via menthone or isomenthone, and direct hydrogenation to the four menthol diastereoisomers) were determined from the changes in composition of the reaction medium during the reaction process. It has been shown that hydrogenation via the menthone intermediates is the major route, the formation of the *cis* isomer (isomenthone) being favoured. The configuration of the menthols, produced from direct hydrogenation or from the ketone intermediates, is controlled by the geometry of adsorption of the precursors on the metal surface, so that neoisomenthol with all substituents in the *cis* position is by far the most abundant stereoisomer produced.

INTRODUCTION

A few years ago, Bartok (*1*) pointed out that the stereochemical approach in heterogeneous catalysis was spreading slowly and was directed more to the acquisition of qualitative information than to fundamental studies involving a complete kinetic analysis of the reaction data. These remarks are relevant as far as the stereoselectivity in the hydrogenation of substituted phenols is concerned. A detailed kinetic analysis of cresol hydrogenation has been carried out (*2–4*), but similar studies are still lacking for other alkylphenols. Thymol hydrogenation has been studied in detail because of its importance for the preparation of menthol. Although several studies have been devoted to improve the selectivity to (±) -menthol (*5–8*), thymol hydrogenation always leads to a mixture of four diastereoisomers so that the industrial processes (*9*, *10*) for the conversion of thymol to menthol rely on multistep separation and recycling operations. Note that an industrial enantioselective synthesis of (−)-menthol has been recently designed starting from myrcene, where the key step is the enantioselective isomerization of geranyldiethylamine into (+)-citronellal enamine on an asymmetric rhodium-BINAP catalyst (*11*). The reduction of menthone–isomenthone mixtures has also been studied in the presence of commercial noble catalysts (*12*, *13*) and of nickel or cobalt catalysts (*14*).

We have started a series of investigations to find out how much and why the stereoselectivity in thymol hydrogenation is affected by the nature of the metal, the morphology of the metal particles, the presence of modifiers, and the nature of the solvent. In this first paper, a kinetic study of thymol hydrogenation has been carried out on a well-characterized platinum catalyst to evaluate the importance of the different reaction pathways. All the reactions were conducted in cyclohexane, an aprotic and nonpolar solvent, to minimize solvent effect.

EXPERIMENTAL

Catalysts

The catalysts were prepared by ion-exchange of an active charcoal (CECA 50 S,

[1]To whom correspondence should be addressed.

0021-9517/93 $5.00

1400 $m^2 g^{-1}$) (*15*, *16*). The support was washed with hot hydrochloric acid to eliminate mineral impurities. It was then functionalized by oxidation with sodium hypochlorite solution (3.5% active chlorine) at room temperature. The ion-exchange was performed by stirring the support under N_2 for 15 h in an ammoniacal solution of $[Pt(NH_3)_4]Cl_2$ (Johnson & Matthey) to a nominal weight loading of 2–7.5%. The suspension was filtered, washed with water until neutrality, and dried overnight in an N_2 atmosphere at 373 K. The reduction was carried out under flowing hydrogen (gas flow rate 0.25 liter min^{-1}) by heating at 1 K min^{-1} from 298 to 573 K, maintaining this temperature for 2 h and cooling to room temperature in the hydrogen stream. The composition of the catalysts was determined by chemical analysis. The size of the metal particles and their distribution in the grains of the microporous active charcoal were determined by transmission electron microscopy (TEM) with a JEOL 100 CX microscope. Thin sections were cut with an ultramicrotome to check whether the metal particles were distributed throughout the active charcoal grain.

Hydrogenation Procedure

The liquid-phase hydrogenations of thymol were performed in a 0.3l autoclave with a magnetic stirrer, using 0.05 mol of thymol and $\approx 0.6 \times 10^{-3}$ mol% platinum relative to the thymol reactant. The catalyst was loaded in the autoclave with 90 ml cyclohexane. After sealing, the autoclave was purged several times with helium, then with hydrogen before setting the required hydrogen pressure. The catalyst was activated by stirring under 3 MPa H_2 pressure at the temperature of the reaction for 2 h. The thymol reactant, dissolved in 30 ml cyclohexane, was heated at the same temperature and introduced into the reaction under H_2 pressure. During the run, the hydrogen pressure was kept constant by continuous feeding from a high-pressure reservoir. Samples of the reaction medium were taken periodically for analysis by gas chromatography (DB WAX, J & W column, 30 m × 0.32 mm; film thickness 0.25 μm). This column, by choosing the appropriate temperature program, gives a good separation of *cis*- and *trans-p*-menthane (*c*-M and *t*-M), menthone (MN), isomenthone (IMN), neomenthol (NML), neoisomenthol (NIML), menthol (ML), isomenthol (IML), and thymol (TH) (Fig. 1).

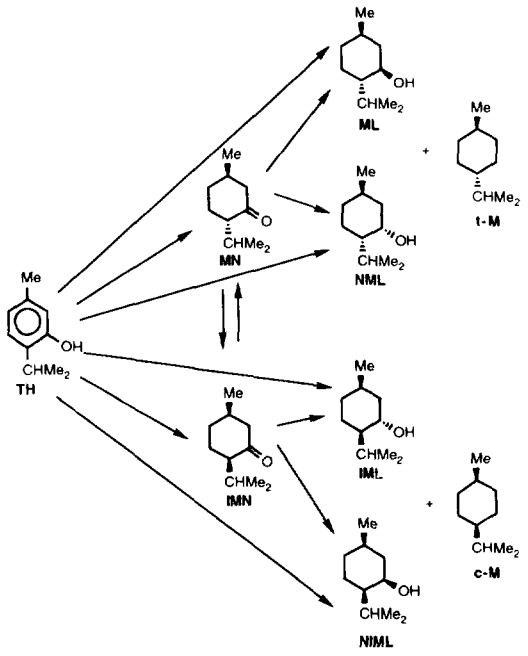

FIG. 1. Products from thymol hydrogenation.

The initial rates of hydrogenation were obtained from the initial slope of the curves giving the thymol concentration as a function of time.

RESULTS AND DISCUSSION

1. Characterization of Catalysts

Catalysts of composition *x* wt% Pt/C, (*x* = 2.63, 4.18, 6.0, and 7.5) were prepared by ion-exchange. Figure 2 shows a TEM view of a Pt/C catalyst after reduction at 573 K. All the particles are in the size range 1–2 nm and are homogeneously dispersed in the grains of the active charcoal, as pre-

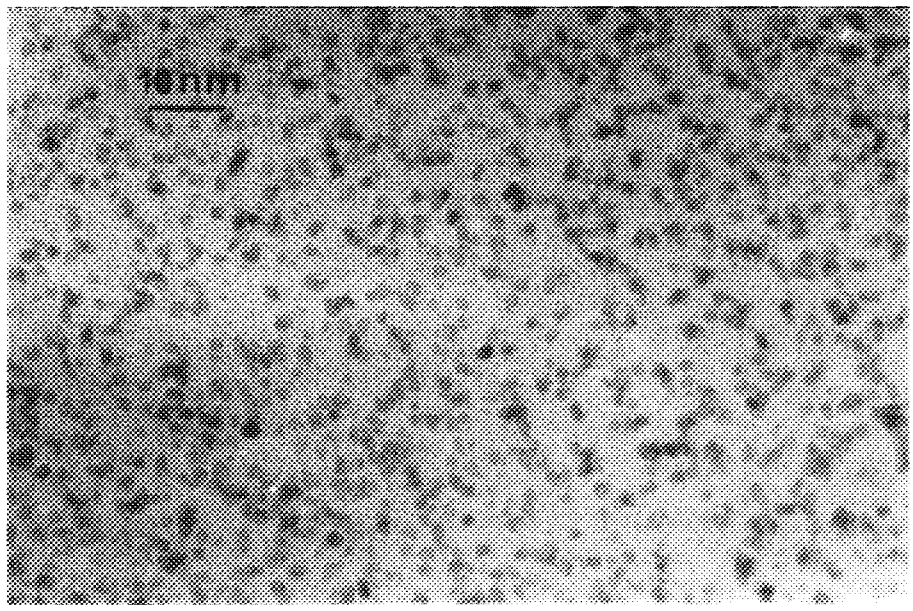

FIG. 2. TEM view through an ultramicrotome section of a Pt/C catalyst.

viously found for this type of preparation (*16*).

2. Preliminary Studies

In the stirred slurry tank reactor used for thymol hydrogenation, the hydrogen has to be transferred from the gas to the liquid phase and then to the catalyst surface on which the reaction takes place. A number of parameters such as speed of agitation and catalyst loading were varied to verify the absence of external diffusion limitations.

It was shown that the hydrogenation rate was independent of the stirring speed of the mixture above 700 rpm, which implies the absence of catalyst agglomeration and of gas-to-liquid mass transfer limitation. The hydrogenation experiments were therefore carried out at $\approx$1000 rpm.

In the kinetic regime, the rate of a catalytic reaction is proportional to the number of catalytic sites and thus to the total metal surface area. To check this proportionality, the surface area of the metal was varied first by increasing the quantity of the 4.18% Pt/C catalyst from 0.1 to 0.25 g and second by using 0.15 g of catalyst with different amounts of metal (2.6 to 7.5%). As previously mentioned, the platinum is always distributed homogeneously within the charcoal particles and the particle sizes are practically the same in the different catalysts. Figure 3 shows that there is a linear relationship between the rate of reaction and both the catalyst loading (curve a) and the metal content (curve b), which is an indication of the absence of external diffusional effects. However, these experiments do not rule out the presence of diffusional effects in the micropores where the metal particles are located. The fact that the curves in Figs. 3a and 3b give a positive intercept on the x-axis tends to prove that a small fraction of the metal is poisoned by impurities in the organic reactant or in the solvent.

3. Product Distribution vs Conversion and Temperature

The hydrogenation of thymol was performed between 313 and 373 K using 0.150

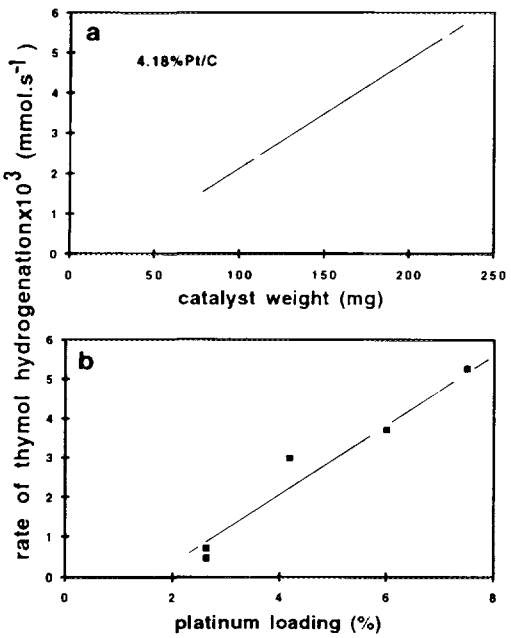

FIG. 3. Rate of reaction (P_{H_2} = 3 MPa, T = 333 K): (a) as a function of catalyst loading (4.18% Pt/C catalyst), and (b) as a function of metal content of the catalyst.

g of the 4.18% Pt/C catalyst. The time dependence of thymol conversion and product formation is shown in Figs. 4a and 4b for two temperatures. At the initial stage of the reaction, a rapid hydrogen consumption is observed; simultaneously, the concentration of thymol decreases while cyclohexanones (IMN and MN) together with cyclohexanols (NIML, NML, ML, and IML) are formed. The thymol concentration then begins to decrease at a lower pace, while the yields of IMN and MN exhibit a maximum. The concentrations of the products of the menthol series increase until all thymol, IMN, and MN are hydrogenated. Some hydrogenolysis also occurs leading to the formation of *cis*- and *trans*-*p*-menthanes. These results are better expressed in terms of the product yields vs percent hydrogenation based on H_2 uptake corresponding to complete reduction, i.e., three molar equivalents per molecule (Figs. 5a and 5b).

At higher reaction temperatures, the maximum yields of IMN and MN increase and occur at a higher degree of conversion of thymol. For instance, at 313 K, the maximum of IMN yield attains 15% at 45% thymol conversion, but at 373 K its value rises to 45% and occurs at 92.5% conversion.

Whatever the temperature, IMN, where the methyl and isopropyl groups are located

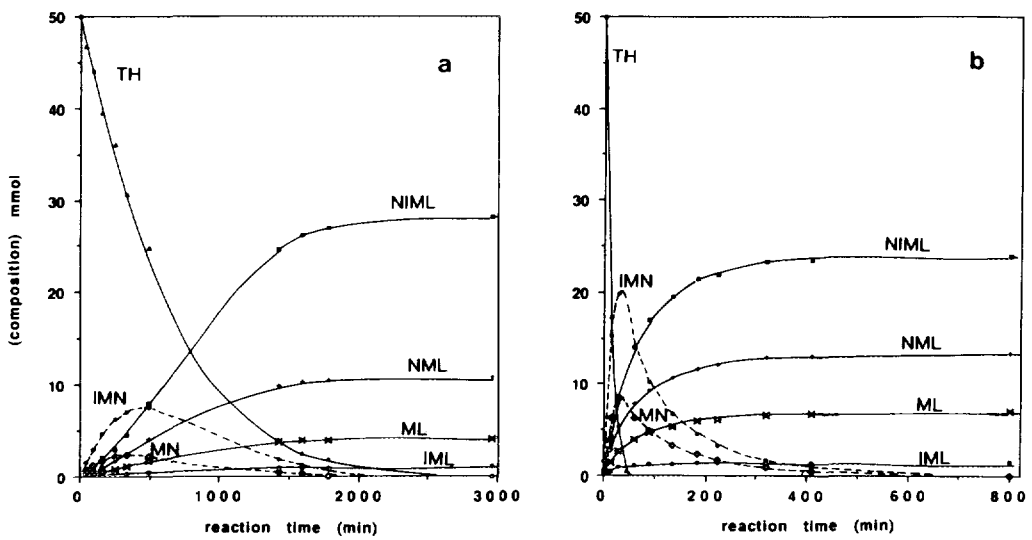

FIG. 4. Product distribution vs time at different reaction temperatures (hydrogenolysis products not represented): (a) 313 K and (b) 373 K.

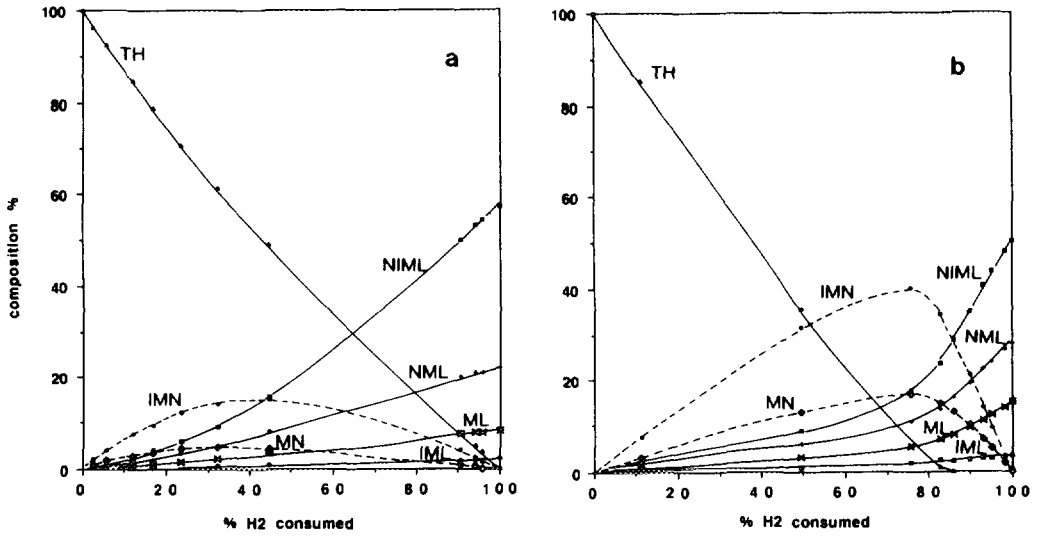

FIG. 5. Product distribution vs percentage of hydrogen consumption at different temperatures (hydrogenolysis products not represented): (a) 313 K and (b) 373 K.

in the *cis* position, is produced preferentially to MN; the initial selectivities (obtained from the initial slopes of the curves giving product yields as a function of conversion) are ≈50% and ≈20%, respectively. The curves giving the product distribution as a function of time (Figs. 4a and 4b) and as a function of conversion (Figs. 5a and 5b) also indicate that the different menthol isomers are detected in the reaction medium as soon as hydrogenation starts; the menthol isomers are produced with initial selectivities NIML ≈ 15, NML ≈ 9, ML ≈ 5, and IML ≈ 1%. Thus, they are not formed exclusively via the hydrogenation of the menthones. However, the initial rates of formation of the menthones, especially of IMN, are much higher than those of the menthols, which suggests that the main reaction pathway involves the intermediate formation of menthones. A similar reaction scheme involving two reaction paths was also suggested by Takagi (*4*) to account for the hydrogenation of isomeric cresols over platinum-metal catalysts. On the other hand, Coussemant and Jungers (*17*) hydrogenated phenol in the liquid phase with a Raney nickel catalyst, and concluded from the analysis of the reaction kinetics that the hydrogenation proceeds exclusively via cyclohexanone.

After complete hydrogenation (of thymol and of the menthones), the menthol isomers coming from isomenthone are the major isomers; the stereoisomeric composition of the alcohols produced follows the series: NIML > NML > ML > IML. However, this series is slightly temperature dependent: any increase in temperature results in a slight decrease in the NIML yield, in favour of the other isomers, as shown in Table 1.

TABLE 1

Product Yields and Effect of Temperature

Temperature (K)	Composition of menthols (%)[a]			
	NIML	NML	ML	IML
313	63.85	24.6	9.15	2.4
333	63.55	24.05	9.9	2.5
353	59.7	26.05	11.4	2.8
373	51.9	29.0	15.6	3.5

[a] At 100% H_2 consumed.

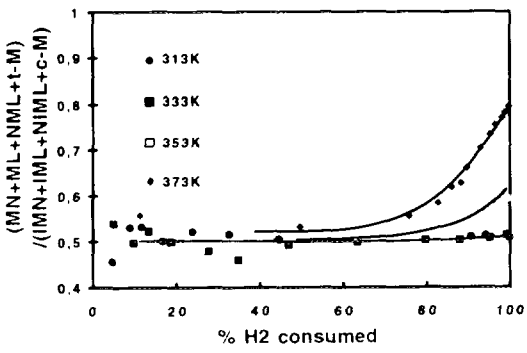

FIG. 6. Ratio of "menthone-type" products to "isomenthone-type" products vs percentage of hydrogen consumption.

To interpret the changes in product distribution with temperature, we first checked that they cannot be due to an isomerization of the different menthols. Figure 3b shows that even at 373 K under hydrogenating conditions, the distribution of the hydrogenated products does not change. We then checked, by hydrogenating a mixture of 70% MN and 30% IMN, that the corresponding alcohols were obtained in the same ratio, namely, MN gave exclusively ML and NML, while IMN gave IML and NIML. A close inspection of the product distribution as a function of the conversion and of the reaction temperature shows that the selectivity changes only at high conversion and above 333 K. Thus Fig. 6 indicates that the ratio

$$(MN + ML + NML + t\text{-}M)/(IMN + IML + NIML + c\text{-}M)$$

remains constant during the whole run at low temperatures but increases at higher temperatures (353–373 K) and when ca. 80% of the H_2 has been consumed, i.e., by reference to Fig. 3b, when nearly all the thymol has been hydrogenated. The change in product distribution could be attributed to an epimerization of IMN into the thermodynamically more stable MN above 333 K and when the metal surface is almost completely free from adsorbed thymol molecules.

The menthol isomer distribution changes as the reaction proceeds, as shown by the curves giving the ML/(NML + ML) and IML/(NIML + IML) ratios as a function of the hydrogen consumption (Fig. 7). There is an increase in the formation of isomers with the "neo" configuration in the course of the hydrogenation. This change can be explained if we assume a different stereoisomeric composition of the menthols depending on whether they are produced directly from thymol or from the menthones. This hypothesis is supported by the results of Takagi (*4*), who found that a higher proportion of *cis* alcohol was produced from methylcyclohexanone than from cresol under the same reaction conditions. Consequently the higher proportion of *cis* isomer formed as the reaction proceeds is due to a higher proportion of alcohol produced via the ketone.

4. Analysis of the Reaction Kinetics

The reaction data have been interpreted using a kinetic analysis with a formalism similar to that used by Cathala and Germain (*18*). The different reaction pathways are described in the simplified scheme given in Fig. 8. Hydrogenolysis products formed in small amounts are not considered. Also,

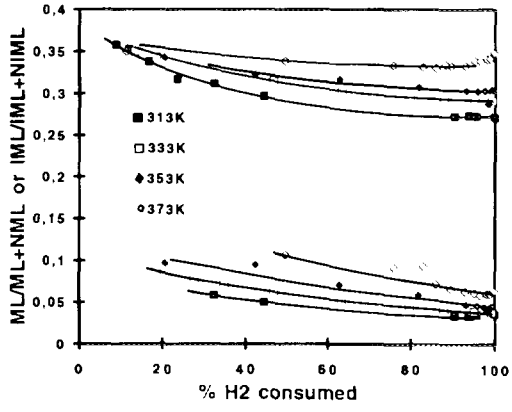

FIG. 7. Relative concentration of *trans* alcohols ML/(ML + NML) (upper series of curves) and IML/(IML + NIML) (lower series of curves) as a function of hydrogen consumption.

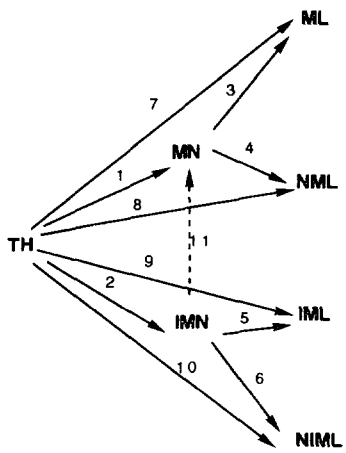

FIG. 8. Thymol hydrogenation scheme.

this scheme does not take into account all the possible intermediate species formed transiently along the various pathways, such as unsaturated alcohols possibly formed in reactions 1, 2, 7, 8, 9, and 10 which would hydrogenate very rapidly.

Reactions 7, 8, 9, and 10 account for the formation of the menthol isomers via the direct route while reactions 1, 2, and then 3, 4, 5, and 6 reflect the intermediate formation of menthones. Reaction 11 corresponds to the epimerization of IMN into MN. As discussed previously, this isomerization occurs only after thymol has been almost completely converted, so it can be neglected, since the kinetic analysis relies only on the reaction data obtained in the region where less than 75% of hydrogen has been consumed. Furthermore, it will be assumed that the alcohols formed at the very first stage of the hydrogenation do not contain any alcohol formed via the ketone intermediates.

Considering pseudo-first-order kinetics with respect to each organic reactant, a system of differential equations independent of time can be obtained. From the initial conditions and from the positions of the maxima of MN and IMN, a set of relative values of the different rate constants (pseudo-first-order constants) has been calculated (see the Appendix). Moreover, the apparent activation energy for hydrogenation of thymol obtained from the Arrhenius plot is found to be 63.5 kJ mol^{-1}. This activation energy corresponds to the disappearance of thymol, represented by the rate constant $k = k_1 + k_2 + k_7 + k_8 + k_9 + k_{10}$. The relative values of k at the different temperatures may then be calculated by the Arrhenius relation setting arbitrarily $k = 1$ at 313 K (see the Appendix). The relative values of the rate constants k_i are then determined; they are given in Table 2.

The probability of the different reaction pathways can be evaluated from a comparison of the relative rate constants. Thus, the proportion of thymol which is hydrogenated to MN and IMN is $(k_1 + k_2)/k = 0.73$. This proportion can be tentatively interpreted by the following reaction mechanism. Let us consider, as Siegel *et al.* did in the case of the hydrogenation of isomeric xylenes (*19, 20*) and as Takagi did in the case of cresol (*4*), that thymol reduction proceeds stepwise via olefinic intermedi-

TABLE 2

Relative Rate Constants for the Different Reaction Pathways of Hydrogenation of Thymol

T(K)	k_1	k_2	k_3	k_4	k_5	k_6	k_7	k_8	k_9	k_{10}
313	0.21	0.52	0.42	1.66	0.03	1.70	0.05	0.09	0.01	0.14
333	0.86	2.11	1.01	3.96	0.12	3.25	0.21	0.39	0.06	0.65
353	3.13	7.89	1.26	3.25	0.13	3.52	0.69	1.31	0.23	2.19
373	10.33	24.85	1.90	3.29	0.14	3.70	2.39	4.47	0.74	6.96

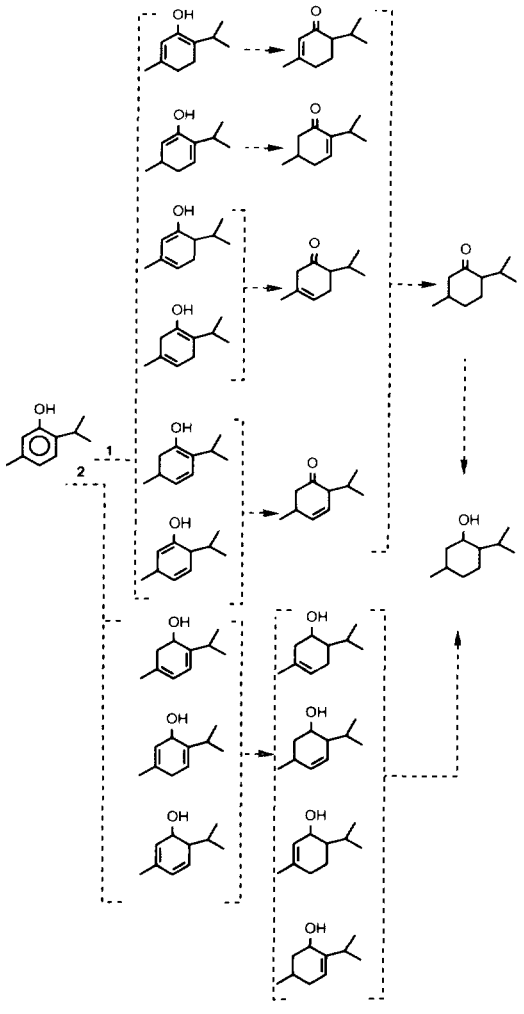

FIG. 9. Tentative scheme for the hydrogenation of thymol to menthols via di- and tetra-hydro intermediates.

ates, with possible desorption and subsequent readsorption and hydrogenation. Let us also assume that all dihydrophenols are formed with equal probability and that saturated ketones will be formed only by hydrogenation of unsaturated ones and by isomerization of enols. These assumptions lead to the reaction scheme given in Fig. 9. It implies that six out of nine isomers, i.e., 67%, will be hydrogenated via a ketone intermediate by path 1. Thus this reaction scheme leads to a proportion of thymol hydrogenated via a ketone intermediate very close to the value of 73% given by the kinetic analysis.

The stereoselectivity of thymol hydrogenation can be evaluated from a detailed inspection of the relative rate constants. A higher selectivity to the isomers where all substituents are in the cis position is always obtained. Thus considering the conversion via the menthones, the fraction of thymol converted to IMN, the *cis* isomer of the menthones, is given by the ratio $k_2/(k_1 + k_2) = 0.71$. More generally the stereoselectivity to products with the "neo" configuration where the OH and isopropyl groups are in the *cis* position is favoured. Thus the fraction of IMN subsequently converted to NIML is as high as $k_6/(k_6 + k_5) = 0.96$, and the fraction of MN converted to NML is $k_4/(k_4 + k_3) = 0.8$. Moreover, as far as the direct conversion of thymol to menthols is considered, there is also a good stereoselectivity to menthol isomers with the *cis* configuration; thus thymol hydrogenated via the direct route (path 2 in Fig. 9) gives 48 and 31% of NIML and NML isomers, respectively. However, the comparison of k_1 and k_2 with k_7–k_{10} shows that thymol hydrogenation via menthone intermediates is by far the most probable route.

The large amounts of *cis* products obtained can be interpreted simply in terms of steric effects on the catalysts surface. Due to steric hindrance, the aromatic ring adsorbs parallel to the metal surface, with its side chains tending to keep away from the surface. The unsaturated ketones or their enols formed on partial hydrogenation of thymol (path 1, Fig. 9) are converted to menthones on further reduction, with formation of mainly the *cis* isomer, i.e., IMN. When isomenthone in the chair configuration approaches the surface, it will tend to adsorb on the surface via the carbonyl group because of a haptophilic effect (*21*), i.e., an interaction between the oxygen atom and surface metal atoms. The adsorption takes place more easily in the least hindered situation, i.e., with the two substit-

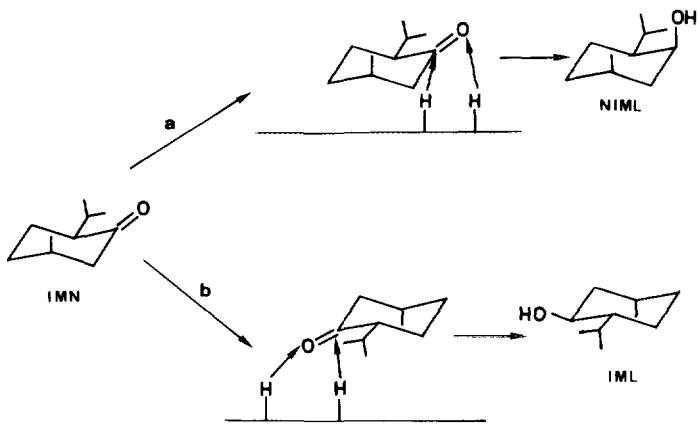

FIG. 10. Steric constraints in adsorption and hydrogenation of isomenthone.

uents away from the surface (intermediate (a), Fig. 10).

The *cis* addition of hydrogen on this preferred adsorbed intermediate yields more probably NIML. A similar explanation may be given for the reduction of menthone which gives a selectivity of 80% to NML, but due to the equatorial position of the methyl group, the steric interactions are less stringent. In the case of the direct hydrogenation of thymol to menthols (path 2, Fig. 9) we observe that the various unsaturated alcohols formed are further hydrogenated to *cis* and *trans* isomers, the *cis* isomer being again the most abundant.

The values of the rate constants corresponding to the reactions from menthones (k_3, k_4, k_5, k_6) increase much less rapidly with temperature than all the other rate constants (Table 2). This is due to a lower value of the apparent activation energy for the hydrogenation of MN and IMN than for the hydrogenation of thymol. Therefore on increasing the temperature, MN and IMN are formed at a higher rate than they are hydrogenated; they accumulate in the medium and they are totally hydrogenated only after complete disappearance of thymol. Similarly, the apparent activation energy for the hydrogenation of 4-methylcyclohexanone on a platinum catalyst was found to be lower than that for the hydrogenation of *p*-cresol (4).

5. *Hydrogenolysis Reactions*

The hydrogenolysis reactions to *para*-menthanes occurred to a greater extent at lower temperatures, attaining 10.25% at 313 K compared to 2.8% at 373 K. These terpenes are formed as long as thymol is present in the reaction medium but their yield remains constant after total conversion of thymol, as shown in Fig. 11.

These results mean that hydrogenolysis takes place probably via allyl-type alcohols

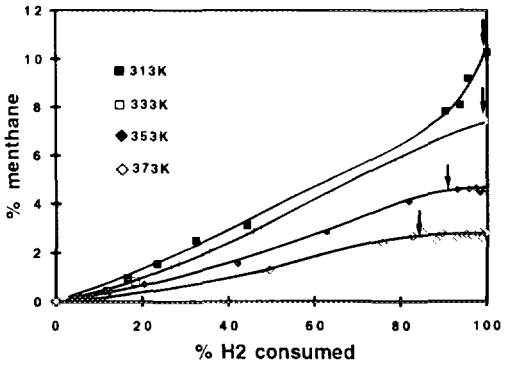

FIG. 11. Hydrogenolysis products vs hydrogen consumption and thymol conversion (100% conversion of thymol given by the vertical arrow).

during the transformation of thymol to the menthones and that menthones are hydrogenated without hydrogenolysis. The yield of hydrogenolysis products is lower at high temperature, although the contrary is expected since the rates of hydrogenolysis reactions increase with temperature. The higher yield at low temperature is due to the prolonged contact time of thymol with the catalyst, e.g., Fig. 4 shows that the contact time is 10 times longer at 373 K than at 313 K.

CONCLUSION

This study is the first attempt to analyze in detail the different reaction pathways of thymol hydrogenation into the four menthol diastereoisomers. From a kinetic analysis of the reaction data at different temperatures on a well-characterized Pt catalyst it was possible to establish the relative probabilities of the hydrogenation routes and thus the stereoselectivity. It is shown that the hydrogenation via ketone intermediates is the preferred route (73%) and that the formation of *cis* isomers is highly favoured. Thus the hydrogenation via the ketones gives 71% of isomenthone which is subsequently hydrogenated with a 96% selectivity to neoisomenthol. The direct route gives 48% of the latter, where all the substituent groups are in *cis* position. Although the *cis* isomers of menthones and menthols are not the thermodynamically more stable stereoisomers, they are formed at comparatively low reaction temperatures because of a stereoselective control by the catalyst.

Indeed, because the thymol molecule is adsorbed with the aromatic ring parallel to the metal surface, the substituent groups tend to keep away from the surface and take a *cis* position upon hydrogenation of the aromatic ring. This mechanism favours the direct formation of neoisomenthol and of isomenthone.

Thus the stereoselective control exerted by the platinum surface disfavours the formation of menthol, which is a target molecule from a mere industrial standpoint. Studies are now in progress to design catalysts leading to a different stereoselectivity.

APPENDIX

In an isothermal stirred batch reactor, for a constant volume of reaction mixture and at constant hydrogen pressure, the following system of differential equations can be written for the different reaction pathways described in the scheme given Fig. 8:

$$dC/dt = k[100 - C] \quad (1)$$

$$dY_{MN}/dt = k_1[100 - C] - (k_3 + k_4)\, Y_{MN} \quad (2)$$

$$dY_{IMN}/dt = k_2[100 - C] - (k_5 + k_6)\, Y_{IMN} \quad (3)$$

$$dY_{ML}/dt = k_7[100 - C] + k_3\, Y_{MN} \quad (4)$$

$$dY_{NML}/dt = k_8[100 - C] + k_4\, Y_{MN} \quad (5)$$

$$dY_{IML}/dt = k_9[100 - C] + k_5\, Y_{IMN} \quad (6)$$

$$dY_{NIML}/dt = k_{10}[100 - C] + k_6\, Y_{IMN}. \quad (7)$$

Here $k = k_1 + k_2 + k_7 + k_8 + k_9 + k_{10}$, $Y_X(\%)$ is the yield in product X, and $C(\%)$ is the conversion of thymol.

After combination with Eq. (1), Eq. (2) may be expressed as

$$dY_{MN}/dC = k_1/k - (k_3 + k_4)/k \times Y_{MN}/[100 - C]. \quad (2')$$

The other equations independent of time (3) to (7) may be obtained similarly. Taking into account the initial conditions ($Y_{MN} = Y_{IMN} = 0$), and the maxima of MN and IMN ($dY_{MN}/dC = dY_{IMN}/dC = 0$), the values of k_i/k can be determined graphically.

The values of k at the different temperatures are calculated by the Arrhenius relation, knowing that the apparent activation energy for hydrogenation of thymol was found to be 63.5 kJ mol^{-1} and setting $k = 1$ at 313 K.

ACKNOWLEDGMENTS

We thank our colleagues, Marc Lemaire, Professor at the Laboratoire de Catalyse et de Synthèse Organique-UCBL, and A. Perrard for helpful discussions.

REFERENCES

1. Bartok, M., "Stereochemistry of Heterogeneous Metal Catalysis." Wiley, New York, 1985.
2. Takagi, Y., Nishimura, S., Taya, K., and Hirota, K., *J. Catal.* **8,** 100 (1967).
3. Takagi, Y., Nishimura, S., and Hirota, K., *J. Catal.* **12,** 214 (1968).
4. Takagi, Y., *Sci. Pap. Inst. Phys. Chem. Res. (Jpn.)* **64,** 39 (1970).
5. Chang, T.-C., and Su, H.-L., *Chung Yuan Hsueh Pao* **6,** 67 (1977).
6. Tungler, A., Máthé, T., Bende, Z., and Petró, J., *Appl. Catal.* **19,** 365 (1985); Tungler, A., Máthé, T., Petró, J., and Tarnai, T., *Appl. Catal. A (General)* **79,** 161 (1991).
7. Repellin, M., Lamartine, R., Perrin, R., and Bertholon, G., *C. R. Acad. Sci. Paris* **285,** 109 (1977); Lamartine, R., Perrin, R., and Bertholon, G., *C. R. Acad. Sci. Paris* **291,** 219 (1980); Lamartine, R., and Perrin, R., *in* "Spillover of Adsorbed Species" (G. M. Pajonk, S. J. Teichner, and J. E. Germain, Eds.), p. 251. Elsevier, Amsterdam, 1983.
8. Bako, P., Fenichel, L., Toke, L., Szente, L. and Szejtli, J., *in* "Proceedings, 4th International Symposium on Cyclodextrins" (O. Huber and J. Szejtli, Eds.), p. 519. Kluwer, Dordrecht, The Netherlands, 1988.
9. Barney, A. L., and Hass, H. B., *Ind. Eng. Chem.* **36,** 85 (1944).
10. Emberger, R., and Hopp, R., *Spec. Chem.* **7,** 193 (1987).
11. Misono, M., and Nojiri, N., *Appl. Catal.* **64,** 1 (1990).
12. Solodar, J., *J. Org. Chem.* **41,** 3461 (1976).
13. Szente, L., Szejtli, J., and Le Tung Chau, *J. Inclusion Phenom.* **5,** 439 (1987).
14. Zubareva, N., Klabunovskii, E., and Kheifits, L., *Izv. Akad. Nauk SSSR, Ser. Khim.* **8,** 1920 (1989).
15. Richard, D., and Gallezot, P., *in* "Preparation of Catalysts IV" (B. Delmon, P. Grange, P. A. Jacobs, and G. Poncelet, Eds.), p. 71. Elsevier, Amsterdam, 1987.
16. Richard, D., de Mésanstourne, R., and Gallezot, P., *in* "19th Conference on Carbon, Extended Abstracts," p. 50. Penn State, 1989.
17. Coussemant, F., and Jungers, J. C., *Bull. Soc. Chim. Belg.* **59,** 295 (1950).
18. Cathala, M., and Germain, J. E., *Bull. Soc. Chim. Fr.*, 4114 (1970).
19. Siegel, S., Smith, G. V., Dmuchovsky, B., Dubbel, D., and Halpern, W., *J. Am. Chem. Soc.* **84,** 3136 (1962).
20. Siegel, S., *in* "Advances in Catalysis and Related Subjects" (D. D. Eley, H. Pines and P. B. Weisz, Eds.), Vol. 16, p. 123. Academic Press, New York, 1966.
21. Rylander, P. N., "Catalytic Hydrogenation in Organic Syntheses," p. 31. Academic Press, New York, 1979.